VERIFICATION OF COMPUTATIONAL MODELS BY COMPARISON OF FINITE-ELEMENT CALCULATIONS AND EXPERIMENTS FOR THE MODEL CASK CASTOR® HAW/TB2

Walter Völzer, Stephan Glutsch, Ronny Perez-Kretschmer, and Pavel Vrastil
GNS – Gesellschaft für Nuklear-Service mbH, Hollestraße 7 A, 45127 Essen, Germany

ABSTRACT

The mechanical analyses in the context of the transport licensing of the type B(U)F package CASTOR® HAW28M Cask for Transport and Storage of Radioactive Material are based upon drop tests with a 1:2 scale model. These tests were accompanied by calculations using Finite Element (FE) analyses.

The purpose of the drop tests was to verify the computational models by comparing numerical and experimental results and to comprehensively study the loading situation of the package under accident conditions with respect to stresses, strains, deformations as well as the kinematical behavior.

For the drop tests under consideration, a 1m pin drop and a 9m slapdown, we observe excellent agreement between experimental and numerical results.

INTRODUCTION

According to the IAEA regulations [1], the integrity has to be proved for Routine Conditions, Normal Conditions which account for minor mishaps, and Accident Conditions. For the cask under consideration with a weight of more than 15 t, a proof for Normal Conditions consists of a 0.6m horizontal drop. For Accident Conditions, a 9m drop onto an unyielding target with arbitrary orientation and a 1m pin drop onto an arbitrary part of the cask need to be considered. The operating temperatures range from −40 °C to a maximum temperature. The latter is determined by a maximum ambient temperature of 38 °C, heat irradiation, and heat production due to the fissile content.

The drop tests were performed from 2005 to 2007 at the Horstwalde drop test facility of the Bundesanstalt für Materialforschung und -prüfung (BAM) [2]. For this purpose, a 1:2 scale model, CASTOR® HAW/TB2 had been built. The aim was to experimentally demonstrate the integrity of the cask and to verify the computational models for the numerical proofs.

The drop tests were preceded by precalculations to identify the locations of maximum mechanical stress, to determine the worst-case orientation for the drop, and to adjust the optimal positions of the

sensors. For those drop tests which were found crucial for the proof of integrity, a recalculation has been performed taking into account the actual temperatures, material properties, and experimental boundary conditions. In contrast, the calculations for the mechanical proofs were carried out for the original cask dimensions, minimum and maximum temperatures, material properties according to Material Specification (usually lower-bound strengths), and idealized boundary conditions.

DROP-TEST PROGRAM

The drop-test program consisted of seventeen drop tests. There were nine 9m drops with various drop orientations (side drop, slapdowns, flat drops, edge drops), seven 1m pin drops on various parts of the cask body or the lid, and a 0.3m side drop to account for Normal Conditions. A schematic drawing of the drop tests is shown in Fig. 1.

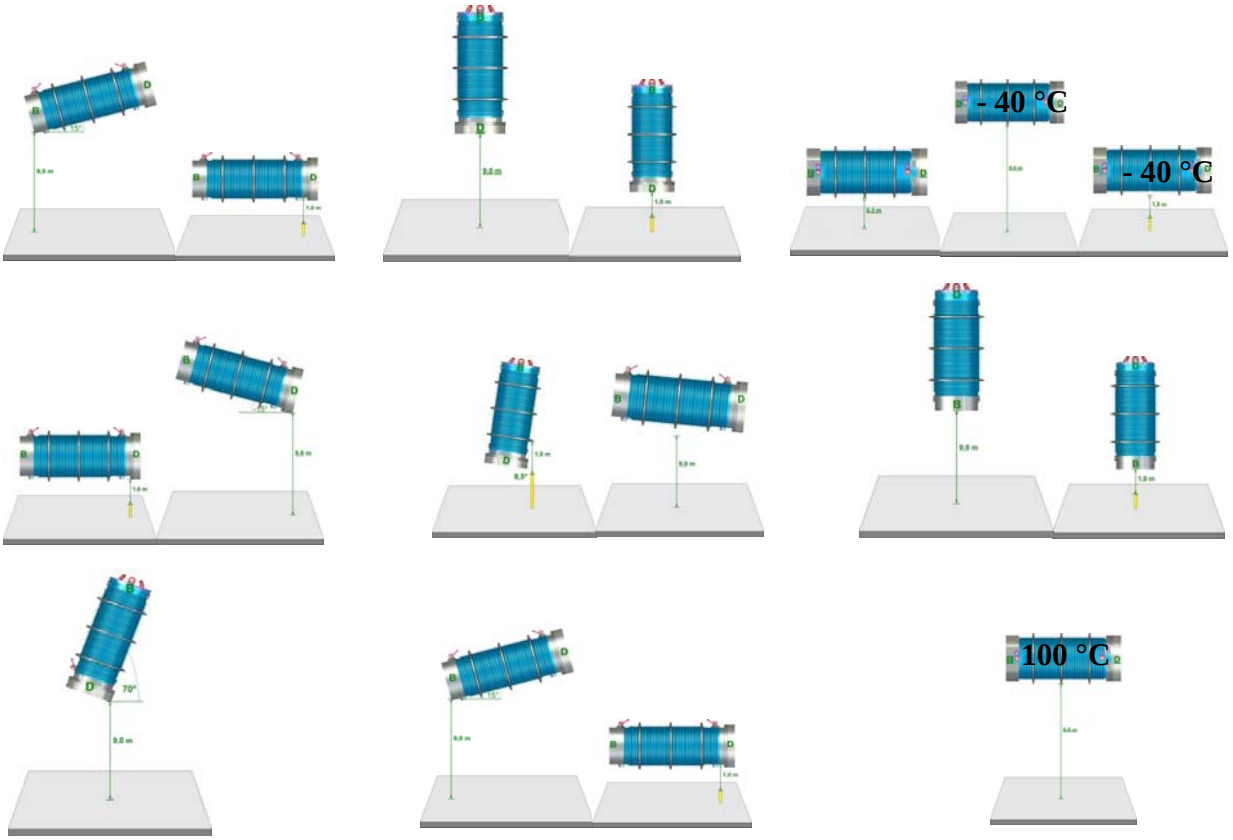

Figure 1. Drop-test program

Several drop tests were performed as sequences in order to account for the accumulation of damages. For example, the third test sequence in the figure consists of a 0.3 m side drop, a 9m side drop, and a 1m pin drop onto the center of the side.

Three temperature ranges have been considered: near room temperature, −40 °C, and about 100 °C to cover the whole range of operating temperatures.

The test specimen was equipped with strain gauges and accelerometers. For each drop test, the active channels were selected according to the precalculated locations of high stresses.

The main aim of the recalculation was to compare experimental and numerical results for the kinematics of the cask, the deformation of components, the strain signals, and the acceleration signals. Furthermore, zones of high stresses or plastic strains were identified. These results served as a basis for the verification of FE models used for the mechanical proofs.

In the next sections, we present results of the recalculation for the following drop tests: a 1m pin drop at the center of the long side at −40 °C and a 9m slapdown with bottom down at near room temperature.

The drop-test program was accompanied by a material test program.

FE MODELING AND DATA ANALYSIS

The FE calculations were done with the explicit FE code LS-DYNA, version 971. For each test or test sequence, a separate model was created to account for the characteristics of each test. For example, submodels with refined meshes were introduced at the impact positions.

The main parts of the specimen are: the cask body, the lid (including lid bolts), a content consisting of model canisters, two trunnions for handling, top and bottom impact limiters made of encapsulated fir wood, and side impact limiters made of aluminum. The test facility consisted of a technically unyielding target (a 220mm steel layer on top of a 5m concrete block [2]) for the 9m drops and a steel bar with socket for the 1m bar drops. For each of these parts, FE models were created and tested separately.

For the cask body, a raw model was built which was later refined for the individual drop tests.

In the experiments, the dynamics of the content was found to be of little influence. Furthermore, the exact locations of the model canisters within the cask were unknown. Therefore, a simplified FE model of the content was created consisting of a homogeneous cylinder with very little stiffness.

For the major parts, the densities of the materials were scaled such that the part masses fit the values in the drawings and the total mass of the model was equal to the total mass of the specimen as determined by weighing.

The FE models have been prepared for the output of time-dependent positions and velocities for selected nodes with a sufficiently high sampling rate in order to calculate the strain and acceleration signals.

Where it was relevant, the drop tests have been calculated as sequences and damping has been applied for a few milliseconds between the individual drop tests.

In Fig. 2, the FE model for the 1m pin drop is shown with a close-up of the impact region.

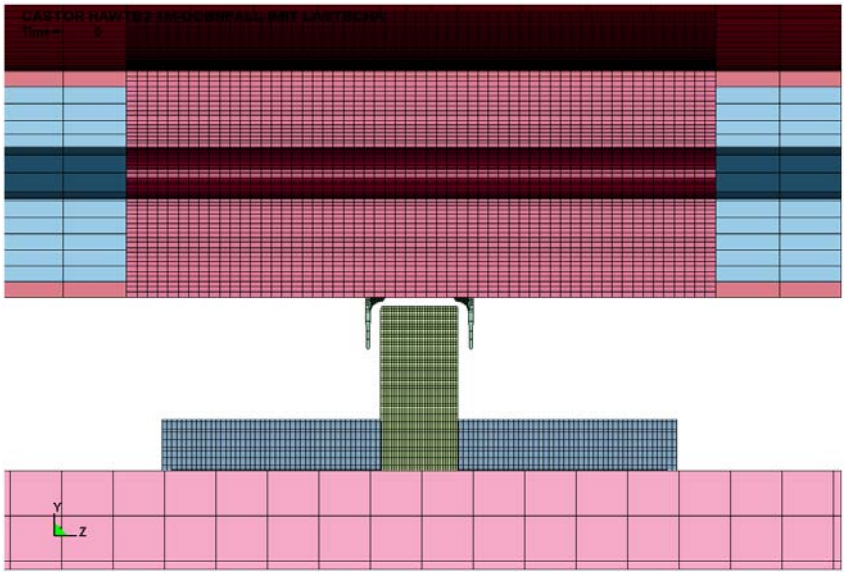

Figure 2. Pin drop, close-up of the impact position

In the FE calculations, various material models have been used: stress-strain curves, in some cases strain-rate dependent, elastic-plastic with tangent modulus, and elastic. The choice was dependent on whether a stress or strain assessment had to be made (cask body) or whether a component undergoes strong deformation (e.g., impact limiters).

The strain signals were computed from the node displacements by interpolation of the displacement field. Both the experimental and numerical signals were filtered by a low-pass filter with a cutoff frequency of 2 kHz.

Due to vibrations, acceleration signals contain strong high-frequency components. In the IAEA Advisory Material [3] it is recommended to choose a cutoff frequency of 100 Hz to 200 Hz for a total mass of 100 t. For the weight of the model cask of 14.6 t, this would result in a cutoff frequency between 190 Hz and 380 Hz. Here, we developed a low-pass filter which preserves maxima and minima such that the maximum deceleration is insensitive to the cutoff frequency in a wide range.

Both experimental and numerical acceleration signals were processed by the same low-pass filter. The acceleration signals from the FE calculations were obtained differentiating the velocities of the nodes at the positions of the accelerometers. Then the accelerations were projected onto the local coordinates to account for a change of the direction when the cask undergoes rotation.

RESULTS

1m pin drop

The deformed steel bar after the drop test is shown in Fig. 3. The experimental result (left) is compared with the result of the calculation. There is a good qualitative agreement and the calculated deformations deviate from the measured ones by less than 10 %.

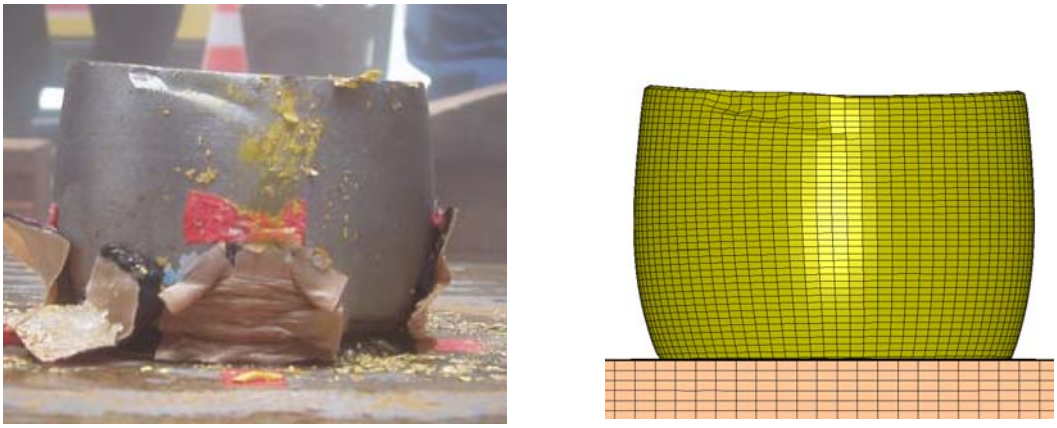

Figure 3. Steel bar after impact. Left: experiment. Right: calculation

The specimen was equipped with a large number of strain sensors. The location of the strain sensors in the neighborhood of the impact position is shown in Fig. 4. The sensors are arranged symmetrically around the nominal impact position. As the experimental impact position deviates from the nominal impact position by a few millimeters, the complementary sensors do not give identical signals.

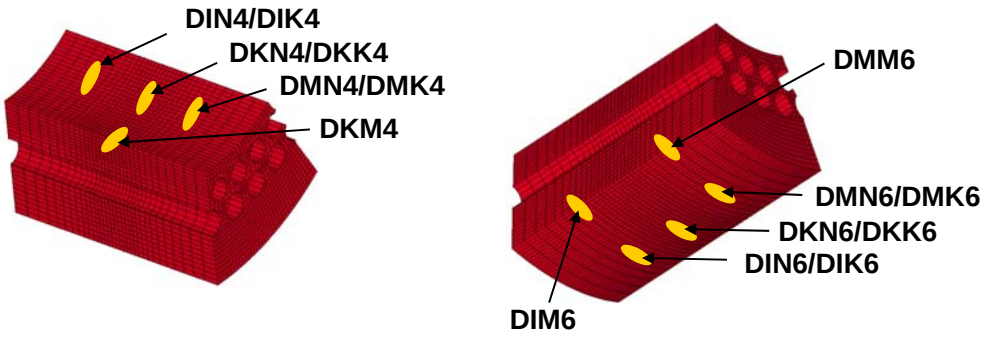

Figure 4. Location of the strain sensors near the impact position on the inside (left) and the outside (right) of the cask body

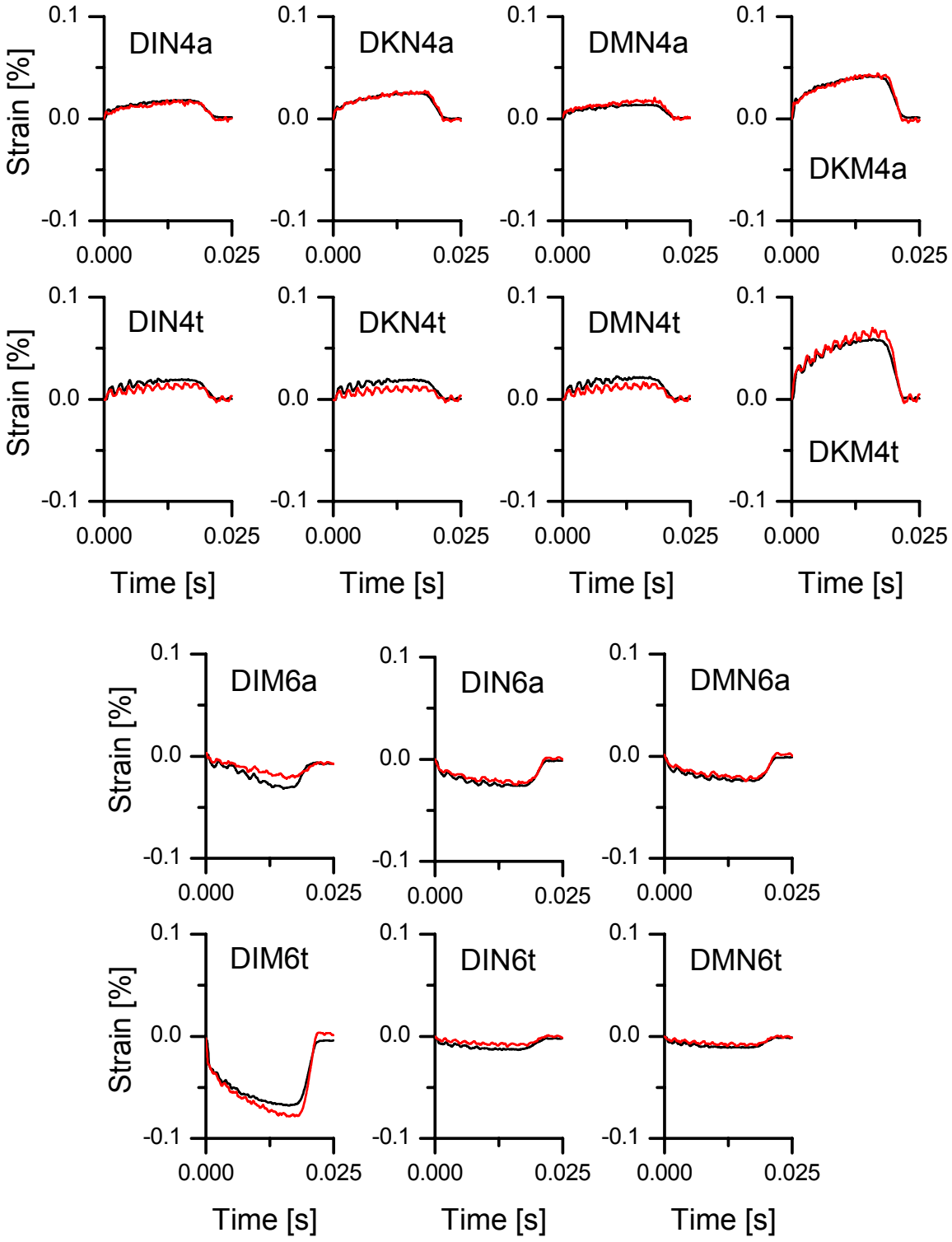

Figure 5. Signals of the strain sensors. Measured values (black curves) are compared with numerical results (red curves)

The signals of the strain gauges near the impact positions are shown in Fig. 5. For each pairs of sensors, only one representative is shown. For each sensor, two signals are displayed corresponding to the axial and tangential direction. The measured signals (black curves) are compared with the calculated ones (red curves). A failure occurred in the signal recording for DKN6 and DKK6 so that these sensors are omitted. The duration of the impact is about 20 ms. The agreement, both qualitatively and quantitatively, between calculated and experimental signals is excellent which evidently proves for the capability of the numerical analysis to reproduce the experimental signals.

9m slapdown

The specimen was equipped with accelerometers at the bottom side (BDG6t), near the center (BMG6t), and at the top side (BSS1t and BTG6t). The acceleration is measured in the direction perpendicular to the cask axis with a positive sign for downward acceleration.

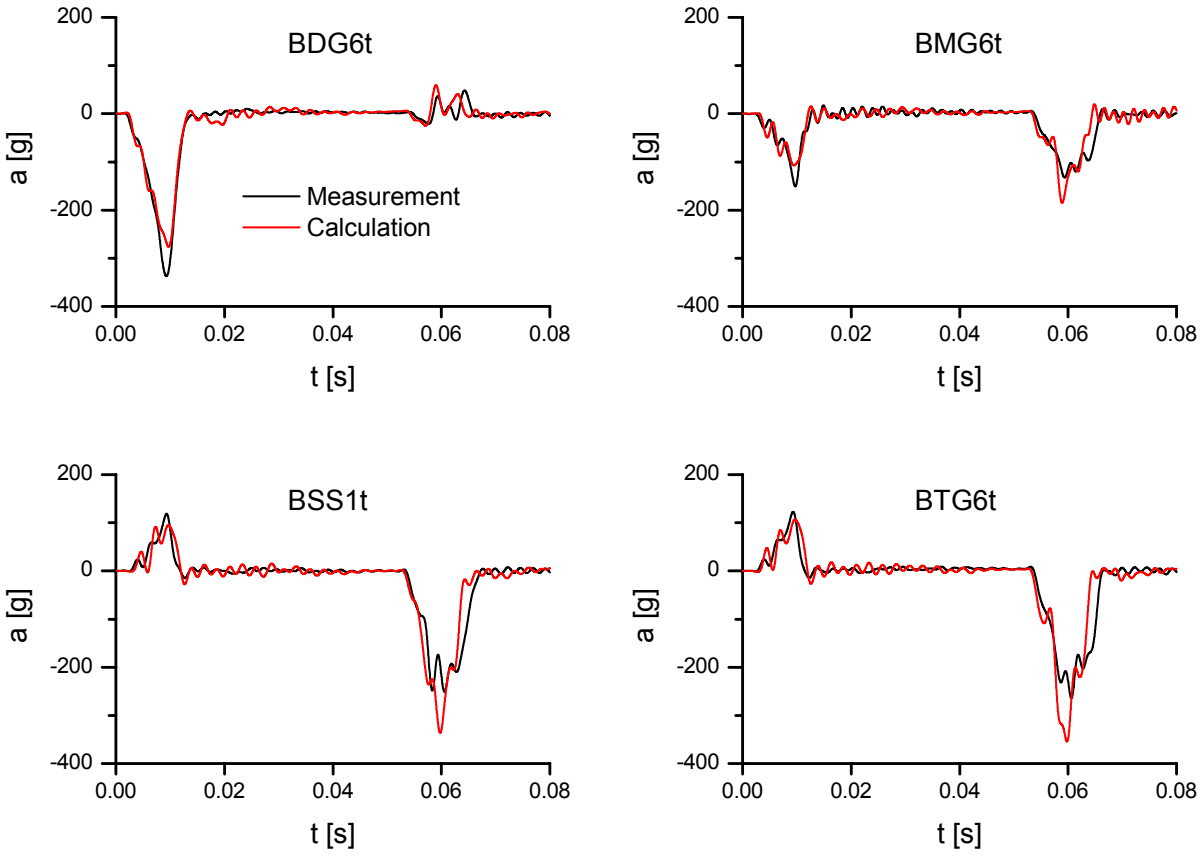

Figure 6. Measured (black curve) and calculated (red curve) acceleration signals

The measured and calculated signals are shown in Fig. 6. All signals show two peaks, one at about 0.01 s and the other at about 0.06 s, which correspond to the primary impact and the secondary impact, respectively. The signs of the peak depend on the location of the sensor. The sensor BDG6t at the bottom gives a strong negative signal for the primary impact and a weak positive signal for the secondary impact. This means that for the secondary impact, the bottom side is subjected to a positive downward acceleration. For the sensors BSS1t and BTG6t at the lid side, the situation is reversed: they first measure an acceleration and then a deceleration. The sensor BMG6t at the center

measures a deceleration both for the primary and the secondary impact. The signal at the center is nearly given by the mean value of the signals from the bottom and the top side.

Both the measured and the calculated signals show small oscillations with a frequency of about 500 Hz which can be identified with the fundamental oscillation mode of the cask. The calculated signal is in good agreement with the measured signal with respect to the positions, widths, and heights of the peaks.

CONCLUSIONS

In summary, GNS has demonstrated that the experimental results for the drop tests can be reproduced numerically with exceptional accuracy with respect to deformations of parts, strain signals and acceleration signals. This was obtained virtually with no adjustable parameters. Therefore, the computational models developed are suitable for the numerical proof of integrity.

ACKNOWLEDGMENTS

The authors are indebted to K. Eberle for comments on the manuscript.

REFERENCES

[1] Regulations for the Safe Transport of Radioactive Material
1996 Edition (As Amended 2003)
Safety Requirements
No. TS-R-1
International Atomic Energy Agency (IAEA), Vienna, 2004

[2] Federal Institute of Materials Research and Testing (BAM)
Drop Test Facility
http://www.bam.de/en/geraete_objekte/fg33_fallversuchsanlage_hw.htm (13.09.2010)

[3] Advisory Material for the IAEA Regulations for the Safe Transport of Radioactive Material
Safety Guide
No. TS-G-1.1 (ST-2)
International Atomic Energy Agency (IAEA), Vienna, 2002